

Impacts of climate change and anthropogenic activities on the normalized difference vegetation index of desertified areas in northern China

MENG Nan, *WANG Nai'ang, CHENG Hongyi, LIU Xiao, NIU Zhenmin

College of Earth and Environmental Sciences, Center for Glacier and Desert Research, Scientific Observing Station for Desert and Glacier, Lanzhou university, Lanzhou 730000, China

Abstract: Vegetation plays a key role in maintaining ecosystem stability, promoting biodiversity conservation, serving as windbreaks, and facilitating sand fixation in deserts. Based on the Moderate Resolution Imaging Spectroradiometer Normalized Difference Vegetation Index (MODIS NDVI) and climate data, a Theil–Sen median trend analysis combined with the Mann–Kendall test and partial correlation and residual analyses were employed to explore spatiotemporal patterns of vegetation dynamics and key drivers in the Badain Jaran and Tengger deserts and Mu Us Sandy Land. Data were collected during the growing season between 2001 and 2020. Further analyses quantified the relative contribution of climate variation and anthropogenic activities to NDVI changes. Results revealed a predominantly increasing trend for average NDVI. The spread of average annual NDVI and growth trends of the vegetation were determined to be influenced by spatial differences. The area with improved vegetation was greater than that of the degraded region. Climate variability and human activities were driving forces controlling vegetation cover changes, and their effects on vegetation dynamics varied by region. The response of vegetation dynamics was stronger for precipitation than temperature, indicating that precipitation was the main climate variable influencing the NDVI changes. The relative role of human activities was responsible for > 70% of the changes, demonstrating that human activities were the main driving factor of the NDVI changes. The implementation of ecological engineering is a key driver of increased vegetation coverage and has improved regional environmental quality. These results enhance our knowledge regarding NDVI change affected by climate variation and human activities and can provide future theoretical guidance for ecological restoration in arid areas.

Keywords: desert; sandy land; vegetation dynamics; climate variation; human activities; relative contribution rate

1 Introduction

With climate change, regional responses, and regional human-earth coupling, terrestrial

Received: 2022-05-15 **Accepted:** 2022-09-30

Foundation: National Natural Sciences Foundation of China, No.41871021

Author: Meng Nan (1996–), PhD, specialized in climate change. E-mail: mengn19@lzu.edu.cn

***Corresponding author:** Wang Nai'ang (1962–), PhD and Professor, specialized in climatic environment change.
E-mail: wangna@lzu.edu.cn

ecosystems are experiencing considerable change (Forzieri *et al.*, 2017; Piao *et al.*, 2020). As a crucial part of ecosystems worldwide, the functions of vegetation are to change the surface conditions, regulate local microclimate, adjust the global carbon balance, and reflect regional human activities (Eastman *et al.*, 2013; Sun *et al.*, 2015; Qu *et al.*, 2020; Wang *et al.*, 2022). Changes in vegetation cover are the direct result of the ecological environment. It is common to use an index to evaluate terrestrial and environmental conditions, especially to measure the degree of desertification (Hellden *et al.*, 2008; Wei *et al.*, 2021). Understanding the dynamic processes and spatial patterns associated with vegetation change and their mechanisms is a critical concern in studies of land ecosystem change (Piao *et al.*, 2015; Du *et al.*, 2019).

Satellite remote sensing-based vegetation indices offer the best method for monitoring spatial and temporal vegetation change regionally and globally (Nemani *et al.*, 2003; Forzieri *et al.*, 2017; Song *et al.*, 2018). NDVI is the most common index for characterizing vegetation growth, which has a positive correlation with vegetation coverage (Tucker *et al.*, 1985; Eastman *et al.*, 2013; Li *et al.*, 2017). In recent years, researchers have monitored vegetation dynamics to identify the driving factors at regional and global scales. The trend of vegetation greening plays a key role at the global scale, especially in the mid-latitude of the Northern Hemisphere, owing to global change (Mynel *et al.*, 1997; Eastman *et al.*, 2013; Piao *et al.*, 2020). Vegetation activity has also been increasing in China (Chen *et al.*, 2019). The synergistic effects of climate variation, namely temperature and precipitation, and anthropogenic factors (Sun *et al.*, 2015; Gao *et al.*, 2019; Jin *et al.*, 2020; Piao *et al.*, 2020) influence vegetation dynamics. There are considerable differences in the response characteristics of Normalized Difference Vegetation Index (NDVI) under different wet and dry conditions and climate change. In ecological regions with limited temperature, climate warming promotes vegetation coverage in temperature-limited areas but can inhibit vegetation growth in arid and semiarid ecosystems with limited water (Mynel *et al.*, 1997; Nemani *et al.*, 2003; Matthias *et al.*, 2015). In most arid areas, a positive correlation exists between vegetation conditions and precipitation, whereas they are negatively correlated with heavy precipitation in humid regions (Nemani *et al.*, 2003; Piao *et al.*, 2015). Human activities are also an important factor in dynamic vegetation change (Qu *et al.*, 2020). Urbanization leads to the conversion of a large area of farm and forest land into construction land. Deforestation results in vegetation reduction and ecological degradation. Ecological engineering construction, active land-use policies, and ecological construction initiatives have contributed substantially to vegetation greening (Yuan *et al.*, 2014; Tian *et al.*, 2021).

Globally, China is among the countries that suffer the most severe desertification damage. The main characteristics of desertification in China are the wide distribution and spanning over a large area (Zhou *et al.*, 2015), which is due to severe drought caused by climate change or damaging human activities, such as overgrazing, deforestation, and poorly planned agricultural reclamation. Desertification reduces the quality of the ecosystem and biological diversity and can also threaten human survival (Wang, 2003). To overcome these problems, China has carried out a series of ecological engineering projects, including the “Three-Norths Shelter Forest Construction Program” and “Grain for Green Project” among others (Li *et al.*, 2013; Yuan *et al.*, 2014; Shao *et al.*, 2017). The large-scale implementation of ecological projects has promoted the improvement of vegetation coverage. Some deserti-

fied regions have undergone reversal of desertification (Guo *et al.*, 2020). The desert areas in northern China account for approximately one fifth of the terrestrial area of the country. They are ecologically fragile and sensitive to climate variation. Many studies have examined variation in the vegetation and the driving mechanisms in this region (Man *et al.*, 2008; Xu *et al.*, 2018; Liu *et al.*, 2019; Wang *et al.*, 2021; Zhao *et al.*, 2021). However, previous studies have not fully established the contribution of climatic factors and anthropogenic activities to vegetation dynamics. It is vital to evaluate the contribution of these two factors and understand the driving mechanisms of ecosystem adaptation and management.

We selected the Badain Jaran Desert (BJD), Tengger Desert (TD), and Mu Us Sandy Land (MUSL) as the study areas. NDVI and climate data were used to assess the spatiotemporal dynamics of the vegetation and explore the impact of climatic change and human activities on changes in the NDVI. These results are potentially useful to learn the interplay among climate, human activities and vegetation variation, as well as provide a scientific basis for further ecological construction and desertification control.

2 Data sources and research methods

2.1 Study area

The BJD (39°04'–42°12'N, 99°23'–104°34'E) is in the northwestern Alax Highland, China. To the south are the Beida Mountains, and to the southeast are the Yabulai Mountains, which separate the range from the Tengger Desert (Figure 1). With an area of approximately 52 000 km², it is the second largest desert in China (Zhu *et al.*, 2010). This desert is well known for its unique landscape of megadunes coexisting with lakes. Under continental climate with an average annual temperature ranging between 9.5 and 10.3°C, it decreases from the north to the south with decreasing elevation (Dong *et al.*, 2004). The average annual precipitation at the northern margin is 35.2–42.9 mm and at the southern margin it is 90.1–115.4 mm. The precipitation is highly concentrated. More than half of the precipitation occurs between May and September, and it is generally dominated by light rain (Ma *et al.*, 2011). The desert vegetation predominantly comprises plant taxa, including *Artemisia ordosica*, *Agriophyllum arenarium*, and *Nitraria tangutorum*.

The TD (37°29'–40°00'N, 102°15'–105°14'E) is the fourth largest desert in China and covers an area of 42,700 km². To the northwest, it is bound by the Yabulai Mountains and to the east are the Helan Mountains (Figure 1). Extensive latticed dunes and more than 420 lakes of various sizes, most of which are saline, are distributed throughout this desert (Zhu *et al.*, 1980). An extreme continental climate controls the TD, with an average annual temperature ranging from 7.5°C in the north to 9.2°C in the south. The mean annual precipitation decreases gradually from the southeast to the northwest. Approximately 70% of the total precipitation occurs from June to September (Zhang *et al.*, 2012). The vegetation is sparse and comprises few species. Most of these are xerophytic, super xerophytic, and halophytic shrubs and semi-shrubs, such as *Haloxylon ammodendron*, *Artemisia desertorum*, and *Caragana korshinskii*.

The MUSL (37°27'–39°22'N, 107°20'–111°30'E) is located in the northern part of the Loess Plateau, with an area of approximately 40,000 km². It has a semi-arid continental monsoon climate. The annual mean temperature ranges from 6.0 to 8.5°C. The average an-

nual rainfall ranges from 250 mm in the northwest and 440 mm in the southeast, where 60%–80% of the precipitation occurs in summer (between June and August) (Wu and Ci, 2002). The main vegetation type in this area is the desert steppes.

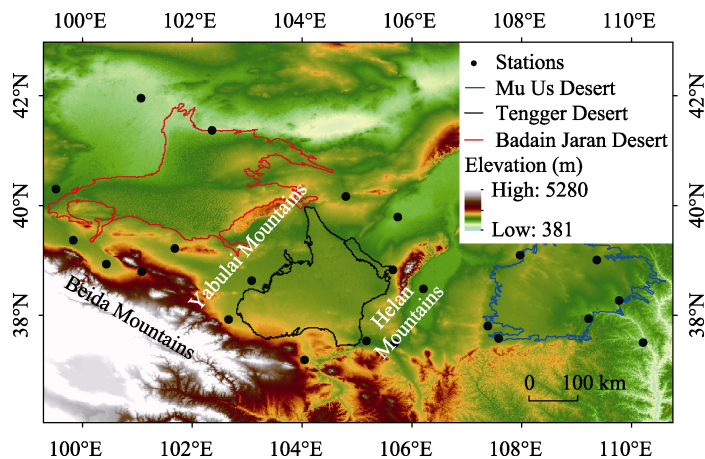


Figure 1 Map of the study region and distribution of the weather stations

2.2 Data sources

2.2.1 NDVI data

The MODIS NDVI dataset provides a high level of spatial resolution and optimal data quality for the examination of water, clouds, and heavy aerosols. This technique has been widely used in the study of regional vegetation coverage change (Justice and Townshend, 2002). MOD13Q1 (a MODIS product, version 6) NDVI data from 2001 to 2020 were derived from the National Aeronautics and Space Administration (NASA) Earth Observing System Data and Information Systems (<http://e4ft101.cr.usgs.gov>). The temporal resolution is 16 days, and the spatial resolution is 250 m. The quality of the data was guaranteed after geometric and atmospheric correction and radiometric calibration. Image mosaic, formatting, and projection transformation of the MODIS data were performed using the MODIS Reprojection Tool (MRT) and Arc GIS 10.3. To reduce atmospheric influence and cloud cover, we used the average monthly mean MODIS NDVI data using the Maximum Value Composition (MVC) method (Holben, 1986). NDVI data between May and September has been defined as NDVI for the growing season. Pixels with NDVI values < 0.1 were excluded (Piao *et al.*, 2011).

2.2.2 Meteorological data

Monthly temperature and precipitation for the surrounding meteorological stations in the three regions between 2001 and 2019 were acquired from the China Meteorological Science Data Center (<http://data.cma.cn>) (Figure 1). The weather data fields were generated with the same spatial resolution and geographic coordinates as the NDVI dataset using kriging interpolation.

The digital elevation model (DEM) data were obtained from the Advanced Spaceborne Thermal Emission and Reflection Radiometer Global Digital Elevation Model (ASTER GDEM) from the Geospatial Data Cloud Platform (<http://www.gscloud.cn>), with a spatial

resolution of 30 m. The desert boundary vector data was derived from the 1:200,000 desert distribution vector data of China Institute of Glaciology and Frozen Desert (<http://www.ncdc.ac.cn/>).

2.3 Methods

2.3.1 Theil–Sen median trend analysis combined with Mann–Kendall test

The Theil–Sen median analysis is a stable non-parametric statistical trend method. This method is insensitive to outliers and does not require the data to follow normal distribution; hence, the general trend in the changing data can be objectively reflected (Sen *et al.*, 1968; Theil *et al.*, 1950), which was calculated as follows:

$$\beta = \text{median} \left(\frac{x_j - x_i}{j - i} \right), \quad \forall j > i, \quad (1)$$

where x_i and x_j are the two variables in the time-series. If β is > 0 , the vegetation is increasing; otherwise, the vegetation is decreasing.

To assess the significance of the variation trend in the vegetation, a non-parametric method, the Mann–Kendall test, was used to reflect the confidence of the changes. It does not need the samples to form a certain distribution and is not disturbed by interference from outliers (Kendall, 1975; Neeti and Eastman, 2011; Liu *et al.*, 2016). The formula for the statistical test is as follows, with a definition of the Z statistic:

$$Z = \begin{cases} \frac{S-1}{\sqrt{\text{var}(S)}}, & S > 0 \\ 0, & S = 0 \\ \frac{S+1}{\sqrt{\text{var}(S)}}, & S < 0 \end{cases} \quad (2)$$

where:

$$S = \sum_{i=1}^{n-1} \sum_{j=i+1}^n \text{sign}(NDVI_j - NDVI_i), \quad (3)$$

$$\text{var}(S) = \frac{n(n-1)(2n+5)}{18}, \quad (4)$$

$$\text{sign}(NDVI_j - NDVI_i) = \begin{cases} 1, & NDVI_j - NDVI_i > 0 \\ 0, & NDVI_j - NDVI_i = 0 \\ -1, & NDVI_j - NDVI_i < 0 \end{cases} \quad (5)$$

n is the length of the time series, $NDVI_i$ and $NDVI_j$ is the data values in time-series i and j ($j > i$), respectively, and $\text{sign}(NDVI_j - NDVI_i)$ is the symbolic function. Under a given level of significance, α , when $|Z_c| > \mu_{1-\alpha/2}$, time-series data represent significant changes at the α level, where $\pm Z_{1-\alpha/2}$ is the standard normal deviation. We used $\alpha = 0.05$; when $|Z_c| \geq 1.96$, the confidence level was $\alpha < 0.05$. The NDVI trend showed significant variation at the 95% confidence level. According to the significance test results, the variation trends were grouped into five grades (Table 1).

Table 1 Classification of the NDVI trend change

β	Z	NDVI trend
$\beta \leq -0.0005$	$Z \leq -1.96$	Significant degradation
$\beta \leq -0.0005$	$-1.96 < Z < 1.96$	Slight degradation
$-0.0005 < \beta < 0.0005$	$-1.96 < Z < 1.96$	Stable
$\beta \geq 0.0005$	$-1.96 < Z < 1.96$	Slight improvement
$\beta \geq 0.0005$	$Z \geq 1.96$	Significant improvement

2.3.2 Partial correlation analysis

As climatic drivers affect vegetation growth simultaneously, the vegetation dynamics are associated with the effects of climatic factors. Partial correlation analysis was used to investigate the relationship between two specific variables. When two variables are associated with a third variable simultaneously, the impact of the third variable is excluded through partial correlation analysis (Li *et al.*, 2013). The formula is as follows:

$$r_{xy \cdot z} = \frac{r_{xy} - r_{xz}r_{yz}}{\sqrt{(1 - r_{xz}^2)(1 - r_{yz}^2)}}, \quad (6)$$

where $r_{xy \cdot z}$ is the partial correlation coefficient between variables x and y after fixing variable z ; and r_{xy} , r_{xz} , and r_{yz} are the correlation coefficients between variables x and y , x and z , and y and z , respectively.

$$r_{xy} = \frac{\sum_{i=1}^n (x_i - \bar{x})(y_i - \bar{y})}{\sqrt{\sum_{i=1}^n (x_i - \bar{x})^2 \sum_{i=1}^n (y_i - \bar{y})^2}}, \quad (7)$$

where r_{xy} is the correlation coefficient, n is the year, x is the mean NDVI in the growing season, and \bar{x} is the mean value of x_i between 2001 and 2019. y_i is the mean temperature or precipitation in the growing season of year i , and \bar{y} is the mean value of y_i between 2001 and 2019. The partial correlation coefficients between NDVI and the climatic factors were analyzed at the 95% level. According to the significance tests results, partial correlations were divided into the following three grades: extremely significant ($p < 0.01$), significant ($p < 0.05$), and non-significant ($p \geq 0.05$).

2.3.3 Residual analysis

To distinguish the influence of climate variation and human activities on vegetation changes, the residual analysis initiated by Evans *et al.* (2004) was used in this study. The main assumption was that the effects of human activities on vegetation change could be represented by inexplicable changes (Evans and Geerken, 2004). In the NDVI climate regression model, temperature and precipitation were selected, which are the climatic factors that most closely correlated with the NDVI. On the basis of this model, the NDVI for each pixel was predicted. The residual value ($NDVI_{HA}$) is the difference between the predicted ($NDVI_{CC}$) and observed NDVI ($NDVI_{OBS}$) values, which illustrates the changes in variation of the vegetation to human activities, calculated as follows:

$$NDVI_{CC} = a \times Pre + b \times Tem + c, \quad (8)$$

$$NDVI_{HA} = NDVI_{OBS} - NDVI_{CC}, \quad (9)$$

where a and b are the regression coefficients and c is the constant term for the regression equation. Tem and Pre represent the temperature and precipitation, respectively. If $NDVI_{HA} > 0$, the impact of human factors is positive $NDVI_{HA} < 0$ indicates reverse effects. The slope of the NDVI slope is calculated as the following equation:

$$slope_{HA} = \frac{n \cdot \sum_{i=1}^n (i \cdot NDVI_i) - \sum_{i=1}^n i \sum_{i=1}^n NDVI_i}{n \cdot \sum_{i=1}^n i^2 - \left(\sum_{i=1}^n i \right)^2}. \quad (10)$$

The relative contribution rates of climate variation and human factors on vegetation change were gained according to Sun *et al.* (2015) and calculated as follows:

$$C_c = \frac{slope(NDVI_{CC})}{slope(NDVI_{OBS})} \times 100\%, \quad (11)$$

$$C_h = \frac{slope(NDVI_{HA})}{slope(NDVI_{OBS})} \times 100\%. \quad (12)$$

2.3.4 Data processing software

MODIS NDVI data were preprocessed on the Google Earth Engine (GEE) cloud platform. ArcGIS 10.3 and MATLAB software were used for statistical analysis.

3 Results

3.1 NDVI spatiotemporal variation characteristics

The inter-annual variation of the average NDVI between 2001 and 2020 was significantly positive in the BJD, with a rate of 0.009/10 a ($p < 0.01$) (Figure 2a1). The NDVI values decreased from the southeast to the northwest. This is consistent with the results of Liu (2016), where the richness and diversity of vegetation species were higher in the southeastern BJD than in the northwestern. The NDVI values were mostly low. Areas with high NDVI vegetation coverage were concentrated in the southeast, around the lakes, and the edge of the oasis or oasis-desert ecotone adjacent to the cities (Figure 2b1). The spatial distribution of the NDVI trend and the mean annual NDVI were the same (Figure 2c1). Substantial spatial heterogeneity was also observed. Areas characterized by improvements were recorded in the southeastern desert area, around the lakes, and along the desert edge (Figure 2d1). In the study area from 2001 to 2020, the spatial area with vegetation improvement was significantly higher (99.98%) than that with the degradation (0.02%). Significantly improved areas, areas with slight improvement, and areas with stable vegetation coverage accounted for 9.36, 1.05, and 89.57%, respectively, of the total area (Table 2). There was little change in the overall pattern of the NDVI. The vegetation growth trend was more pronounced in the southeastern desert area, which was related to the high precipitation in the southeast and abundant underground water resources provided by the lakes.

The NDVI significantly improved during the growing season, with a linear tendency of 0.028/10 a ($p < 0.01$) in the TD (Figure 2a2). The areas with high NDVI vegetation coverage were found in the southeastern, northeastern, southwestern, and central desert sec-

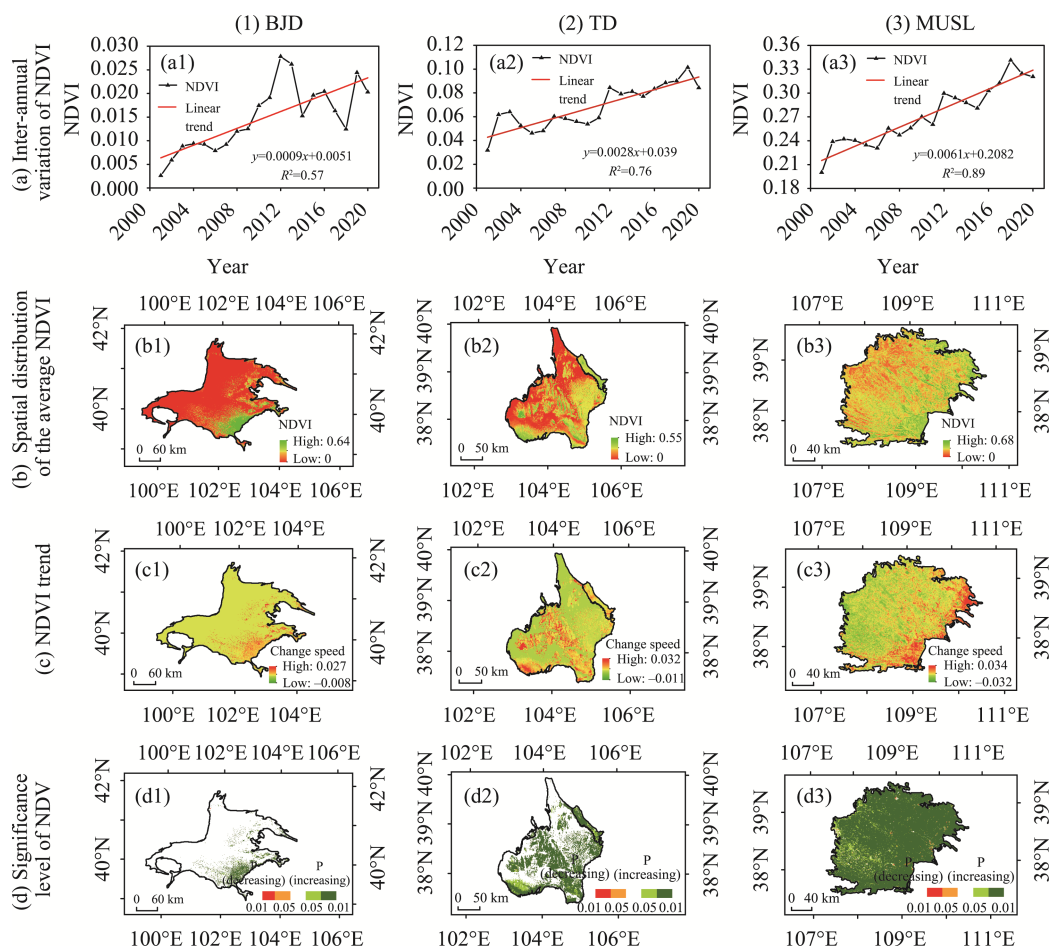


Figure 2 Trends in the NDVI in the growing season from 2001 to 2020 in the Badain Jaran Desert, Tengger Desert, and Mu Us Sandy Land: (a) inter-annual variation in the NDVI, (b) spatial distribution of the average NDVI, (c) annual trends in the NDVI, and (d) five variation levels in the NDVI trends. P (decreasing) and P (increasing) express the P values of the NDVI change, which were stratified into five types: $p < 0.01$ (significant improvement), $0.01 < p < 0.05$ (slight improvement), $p > 0.05$ (stable), $0.01 < p < 0.05$ (slight degradation), and $p < 0.01$ (significant degradation).

tions. The NDVI values increased from the northwest to the southeast (Figure 2b2). Areas of increased vegetation were primarily distributed in the southeastern, southwestern, northeastern, and central sections of the TD (Figures 2c2 and 2d2). The increased trend of vegetation coverage encompassed 48.33% of the total region and 51.57% of stable vegetation coverage. The proportion of the area with an improvement in vegetation coverage was significantly higher than that of the area of degradation (Table 2).

The NDVI of the MUSL exhibited an increasing trend, and the NDVI trend rate was 0.061/10 a (Figure 2a3). The vegetation conditions were better in the eastern region compared to those in the western region, which conforms to the physical geographical areas. In the eastern seasonal wind area, the vegetation has adequate water-heat conditions and the weather conditions are more appropriate for plant life. Therefore, the NDVI was higher. Areas with high NDVI were mainly concentrated in Shenmu County, Yulin District, Hengshan

County, and Dingbian County, forming a mosaic distribution pattern with a low-value cloud (Figure 2b3). The NDVI trend was higher in the eastern and southern areas than in the northern and central regions (Figure 2c3). The significance test for the NDVI trend analysis indicated that vegetation restoration covered almost the entire area of MUSL. Areas of improvement accounted for 89.39% and were located in central and eastern China and between the hinterland mobile sand belt. In the western Ordos desert steppe area, the change in the NDVI was not significant. Less than 2% of the image cloud NDVI showed a degradation trend and the distribution was sporadic (Figure 2d3).

Table 2 Results for the variation in NDVI trends

NDVI trend	Badain Jaran Desert		Tengger Desert		Mu Us Sandy Land	
	Area (km ²)	Percentage (%)	Area (km ²)	Percentage (%)	Area (km ²)	Percentage (%)
Significant degradation	6.00	0.01	8.94	0.03	59.06	0.16
Slight degradation	4.63	0.01	25.13	0.07	243.13	0.66
Stable	42557.38	89.57	17382.88	51.57	537.94	1.46
Slight improvement	500.19	1.05	1981.94	5.88	3076.82	8.33
Significant improvement	4446.75	9.36	14308.56	42.45	33006.50	89.39

3.2 Analysis of vegetation NDVI change influencing factors

3.2.1 Partial correlation between NDVI dynamics and climate change

Hydrothermal conditions are important abiotic factors that determine the spatial distribution and temporal variation of vegetation. Warming and wetting trends have become apparent over the last 20 years in the BJD (Figures 3a and 3b). Partial correlation coefficients between the NDVI, temperature, and precipitation were calculated grid by grid, followed by a significance test (Figures 3c–3f). Findings showed that the effects of the climate factors on variation in the vegetation had considerable spatial heterogeneity. The correlation of the NDVI with temperature was both positive and negative. There was no significant association between the NDVI and temperature, demonstrating that the temperature change had no significant effect on changes in the vegetation. Approximately 1.7% of the area exhibited a significantly negative correlation coefficient between the NDVI and the temperature (Table 3). Rising temperatures are an obstacle for vegetation growth through increasing water evaporation, likely leading to a decrease in soil moisture, which can restrict photosynthesis and the growth velocity of plants (Wang *et al.*, 2010). The area with a significant positive correlation accounted for 19.4% between the NDVI and precipitation, and were distributed in the southeastern and marginal areas of the desert. Therefore, increased precipitation can promote plant growth. The relationship between the NDVI and temperature was less than between the NDVI and precipitation, indicating that precipitation was the main climatic factor influencing vegetation changes in the BJD over the 20-year test period.

The average yearly temperature and precipitation of the TD increased at 0.0368 °C/a and 0.8405 mm/a, respectively (Figures 4a and 4b). Warming and wetting trends were also observed. The area with a significant positive correlation between the NDVI and temperature accounted for 17.6% of the TD, mainly distributed in the center of the desert (Figures 4c and 4d; Table 3). Areas with significant positive correlation between the NDVI and rainfall (28.5%) were distributed in the southwestern, southeastern, and northeastern margins of the desert

(Figures 4e and 4f, Table 3), having a pronounced effect on changes in the vegetation.

The average annual temperature and precipitation in the MUSL followed a growing trend, with changes at 0.0005 C/a and 2.215 mm/a (Figures 5a and 5b). The climate of the MUSL tended to be hot and humid. In the MUSL, 56.9% of the area had a positive correlation while 43.1% of the area had a negative correlation coefficient between temperature and annual NDVI. Less than 1% of the pixels passed the significance level test ($p < 0.05$) (Figures 5c and 5d; Table 3), which were scattered in the center of the MUSL. The results indicated that the NDVI and temperature in the MUSL were not significantly correlated. Moreover, 96.4% of the MUSL had positive correlation coefficients between the precipitation and the annual NDVI, wherein 14.2 and 6.4% of the pixels had p -values of < 0.05 and < 0.01 , respectively. They were mainly distributed in the northwestern, western, and southern sections of the MUSL (Figures 5e and 5f; Table 3). Vegetation growth was more closely related to precipitation than to temperature.

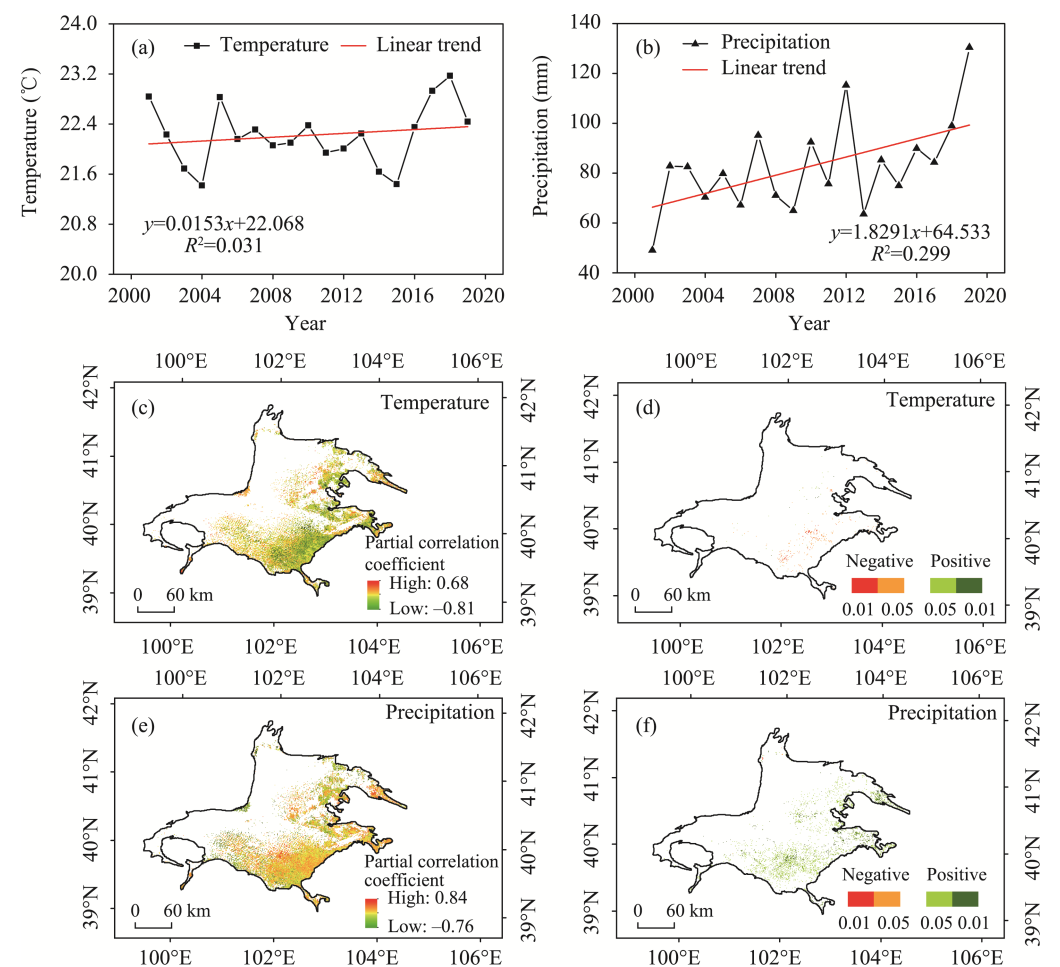


Figure 3 Trends in the temperature and precipitation from 2001 and 2019 and their relationships with the NDVI in the Badain Jaran Desert: (a) inter-annual variation in temperature during the growing season; (b) inter-annual variation in precipitation during the growing season; (c) spatial distribution of the partial correlation between the NDVI and temperature; (d) significance test for the correlations; (e) spatial distribution of the correlation between the NDVI and precipitation; and (f) significance test for the correlations.

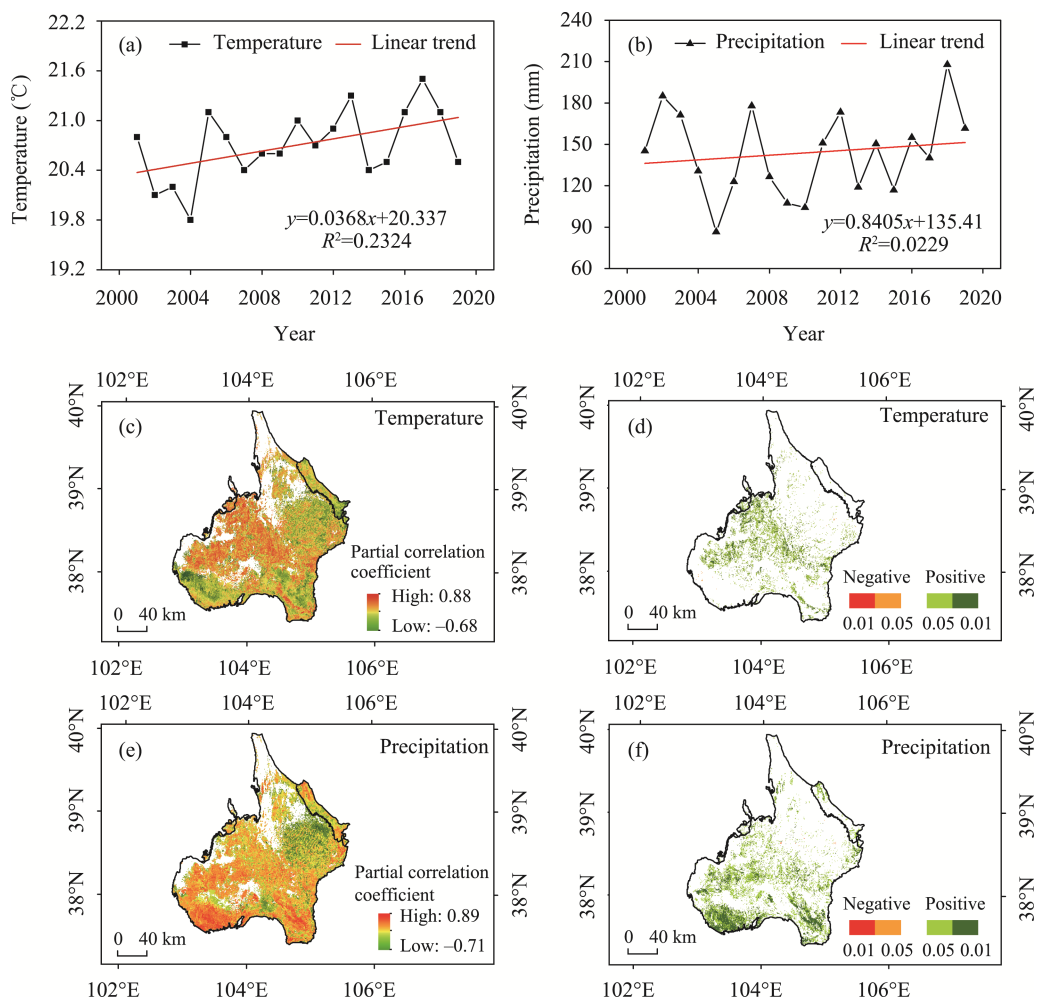


Figure 4 Trends in the temperature and precipitation from 2001 to 2019 and their relationships with the NDVI in the Tengger Desert. The names of (a), (b), (c), (d), (e), and (f) were the same as in Figure 3.

3.2.2 The relative role of climate changes and human activities on vegetation changes

Excluding climatic variables, the impacts of anthropogenic activities on vegetation coverage were also significant. Studying the effects of anthropogenic factors on variation in the vegetation is key for improving management practices for vegetation ecosystems. In the present study, using the residual method to remove the effect of precipitation and temperature on the NDVI, the vegetation status as a result of human activities was obtained. The NDVI residuals showed an increasing trend from 2001 to 2019 in the BJD ($p < 0.01$), with an annual rate of change of 0.01/10 a (Figure 6a). The trend for the NDVI residuals was similar to the spatial distribution of the NDVI trend observed through remote sensing (Figure 6b). Results from the residual analysis indicated that the variation in the NDVI could not be explained only by climate change. Anthropogenic activities have played an important role in enhancing vegetation recovery in the BJD. The trend analysis and significance test were combined to show that the percentage of human activities contributing to the increase in vegetation accounted for 38.0%, which was mainly in the southeastern and marginal areas of the

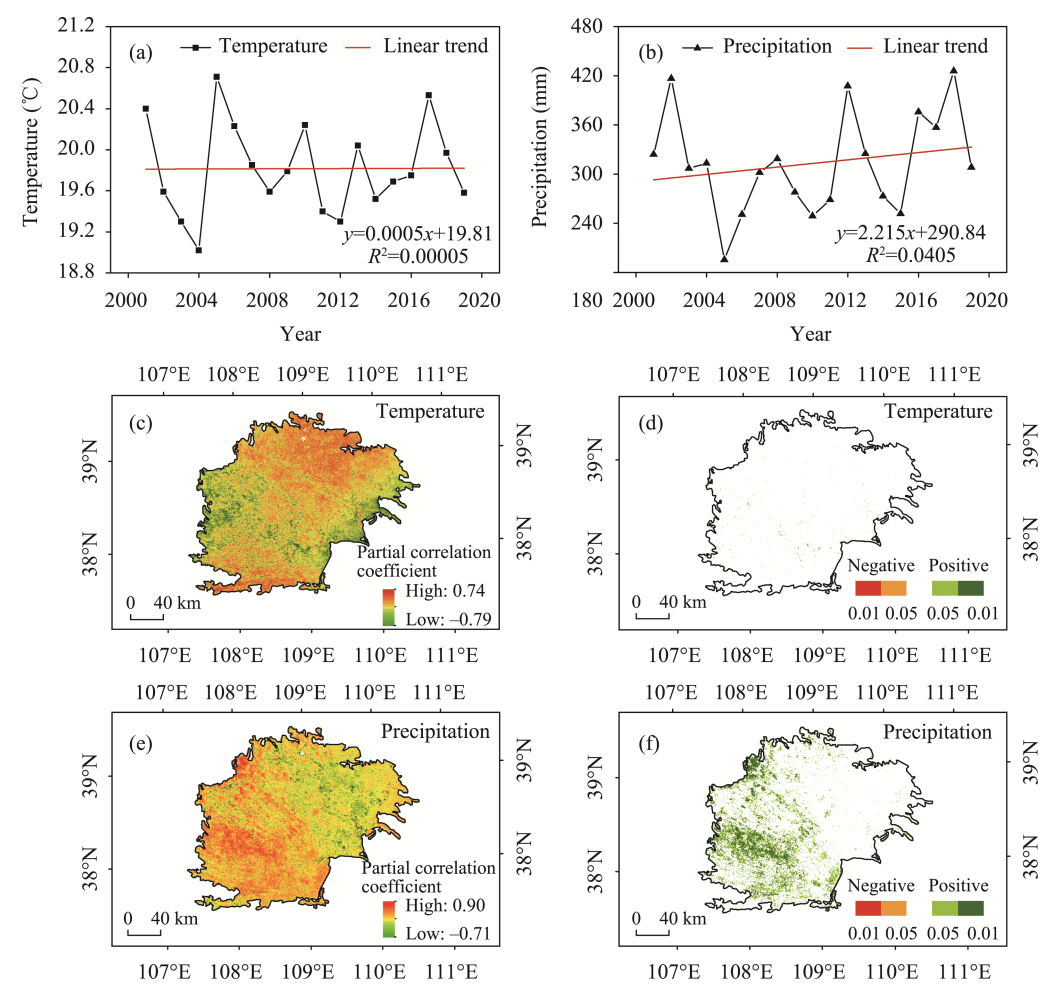


Figure 5 Trends in the temperature and precipitation from 2001 to 2019 and their relationships with the NDVI in the Mu Us Sandy Land. The names of (a)–(f) were consistent with Figure 3.

Correlation	Badain Jaran Desert				Tengger Desert				Mu Us Sandy Land			
	Area (km ²)		Percentage (%)		Area (km ²)		Percentage (%)		Area (km ²)		Percentage (%)	
	Tempe- rature	Precipi- tation	Tempe- rature	Precipi- tation	Tempe- rature	Precipi- tation	Tempe- rature	Precipi- tation	Tempe- rature	Precipi- tation	Tempe- rature	Precipi- tation
Extremely significant negative	62.81	5.06	0.42	0.03	2.00	1.25	0.008	0.005	10.44	3.00	0.028	0.008
Significant- ly negative	186.94	2.38	1.25	0.02	20.94	9.56	0.077	0.035	122.25	18.31	0.332	0.050
No Signifi- cant	14607.13	11999.56	98.02	80.52	22272.19	19316.50	82.280	71.361	36689.44	29252.88	99.573	79.391
Significant- ly positive	36.75	2316.88	0.25	15.55	3757.00	5145.88	13.879	19.010	22.69	5225.25	0.062	14.181
Extremely significant positive	8.00	577.63	0.06	3.88	1016.69	2595.63	3.756	9.589	1.75	2347.13	0.005	6.370

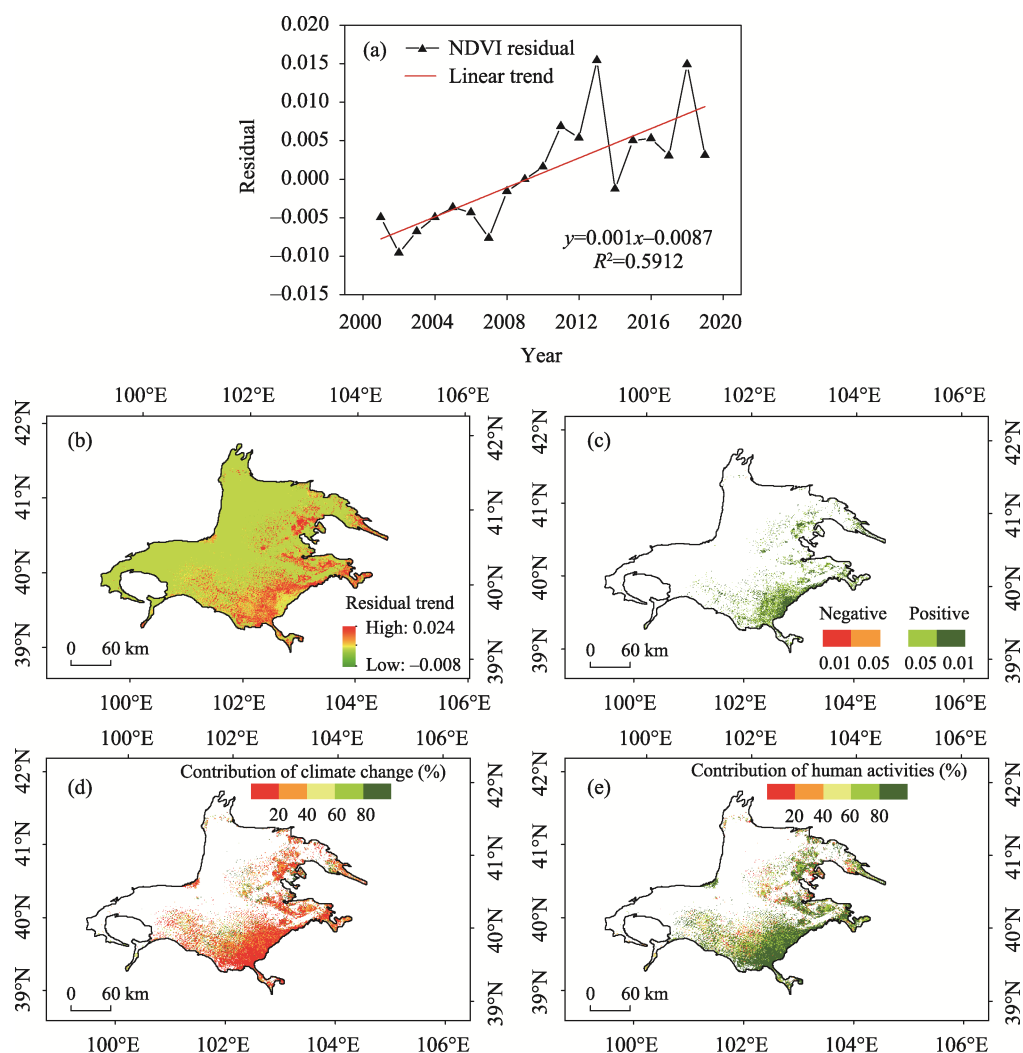


Figure 6 Spatiotemporal distribution of the NDVI residuals across the Badain Jaran Desert between 2001 and 2019: (a) inter-annual variation in the NDVI residuals; (b) spatial distribution pattern of the NDVI residual trend; (c) significance test results for the trend of the NDVI residuals, and spatial distribution of the contribution rate of (d) climate change and (e) human activities to improvement in vegetation coverage.

BJD (Figure 6c and Table 4). Owing to the small area of vegetation degradation, only the relative contribution of these two driving factors was considered as factors for the increase of vegetation. Figures 6d and 6e indicate the relative contribution distribution of the climatic change and anthropogenic activities in the BJD. The relative contribution rate of climate change to the increase in NDVI was relatively high, in the range of 0–20%, which was greater than 50% of the total area. The relative contribution rate of climate change ranging from 80% to 100% accounted for 8.1% of the total area. The contribution of human activities was high in the 60%–80% and 80%–100% regions, accounting for 25.7% and 49.1%, respectively (Figure 6d and Table 5), consistent with the results reported by Jin *et al.* (2020). The average relative contribution of climate change and human elements to variability in NDVI were 28.1% and 71.9%, respectively, demonstrating that human activities are the

principal factors affecting vegetation cover in the BJD.

The NDVI residuals showed an increasing trend in the TD, with rates of change of up to 0.02/10 a ($p < 0.01$) (Figure 7a), in line with those of the NDVI based on remote sensing observations (Figure 7b). The percentage of human activities contributing to the increase in the NDVI accounted for 55.9% in the southeastern, southwestern, northeastern, and central areas of the desert (Figure 7c and Table 4). On the southern edge of the TD in Gansu, Ningxia, and other provinces along the river, the terrain is flat and open with a large area of farmland that is irrigated annually. Since 2003, the local forestry and grass departments have implemented ecological engineering construction along the northeastern edge of the TD. In the spring of 2012, aerial seeding and afforestation projects with artificial planting were conducted in some areas. By 2018, 813,000 mu of artificial vegetation had been restored (Zhao *et al.*, 2021). The felling measures along the southwestern margin have pro-

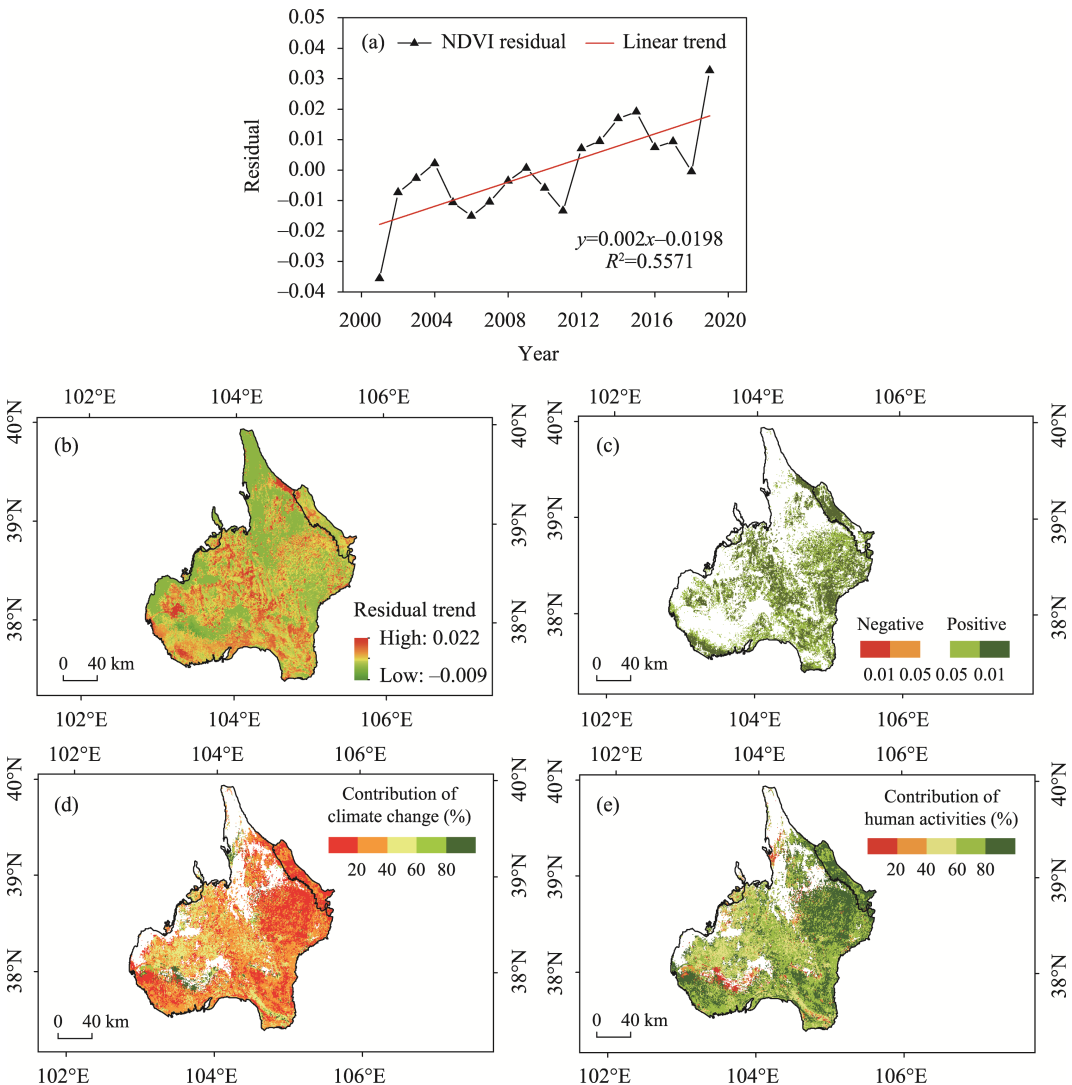


Figure 7 Spatiotemporal distribution of the NDVI residuals across the Tengger Desert between 2001 and 2019. The names of (a)–(e) were consistent with the names in Figure 6.

moted vegetation restoration (Man *et al.*, 2008). The findings of the research correspond with the areas affected by human activities in these regions. The contribution of climatic factors to the increase in NDVI was high in the 0–20% and 20%–40% regions, accounting for 35.3% and 42.1%, respectively. In contrast, human activities were significant in the 60%–80% and 80%–100% regions, accounting for 41.6% and 31.9%, respectively (Figure 7d and Table 5). The average relative contribution of climatic change and human factors to NDVI change were 28.9% and 71.1%, respectively. Based on the rate of the relative actions, it was concluded that human activities played a greater role in vegetation than climate change did. The implementation of large-scale ecological engineering has enhanced the ecological environments in various regions.

The general change in the residual NDVI in the MUSL increased ($p < 0.01$), and the growth rate was 0.054/10 a (Figure 8a). The high residual trend was mainly concentrated in the east (Figure 8b). The contribution of human activity to the increase in vegetation was

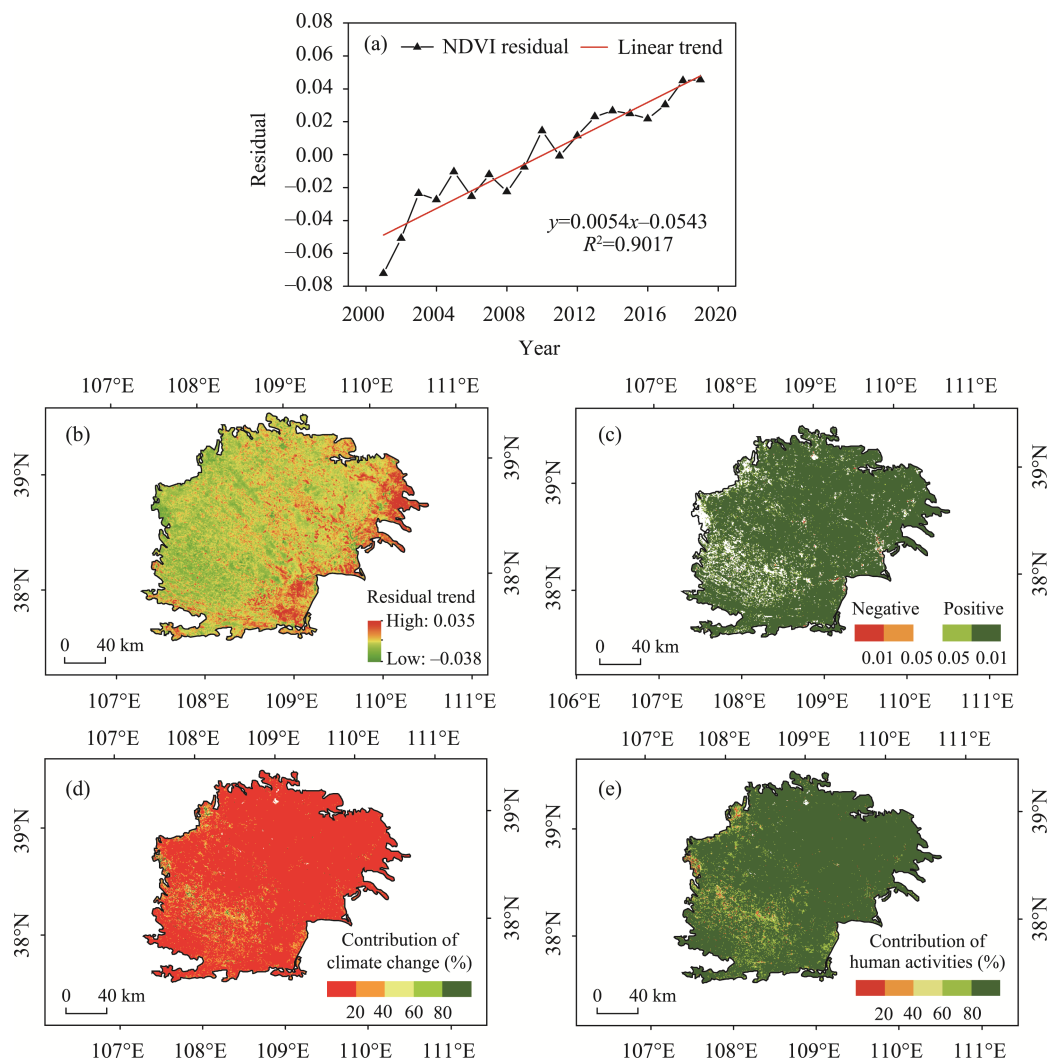


Figure 8 Spatiotemporal distribution of the NDVI residuals across the Mu Us Sandy Land between 2001 and 2019. The names of (a)–(e) were the same as those used in Figure 6.

90.5%, distributed in the eastern part of the MUSL (Figure 8c and Table 4). In contrast, precipitation mainly contributed to the NDVI in the southern and western parts of the MUSL, indicating that the relative effects of climate variation and human activities on changes in the vegetation in the MUSL had considerable spatial variability. Climate variation (relative role in the 0–20% region) accounted for 90% of the changes. The areas where the relative contribution of human activities was > 80% were widespread, 88.7% of which ranged from 80%–100% (Figure 8 and Table 5). The mean contribution rate of climatic factors and anthropogenic activities to the variability in the NDVI was 11.1% and 88.9%, respectively, suggesting that human activities exerted a greater influence on vegetation across the MUSL than that by climate change did. In the 21st century, the Grain for Green Project and more recent biological and engineering measures, such as aerial seeding afforestation, sand area sealing, large-scale afforestation projects, and “grazing ban, grazing rest, rotational grazing,” have been successively and efficiently implemented in the MUSL.

Table 4 Statistics on the significant effects of human activities on vegetation change

NDVI trend	Badain Jaran Desert		Tengger Desert		Mu Us Sandy Land	
	Area (km ²)	Percentage (%)	Area (km ²)	Percentage (%)	Area (km ²)	Percentage (%)
Significant degradation	0.75	0.005	0.8125	0.003	53.5625	0.15
Slight degradation	3.5	0.023	3.75	0.014	38.3125	0.11
Stable	9231.5	61.951	11922.125	44.044	3391.3125	9.20
Slight improvement	2898.6875	19.452	8148.3125	30.102	1969.5	5.34
Significant improvement	2767.0625	18.569	6993.6875	25.837	31393.6875	85.20

Table 5 Statistics on the contribution of two factors (climate change and human activities) to improvement in vegetation coverage between 2001 and 2019

Contribution (%)	Badain Jaran Desert		Tengger Desert		Mu Us Sandy Land	
	Climate change	Human activities	Climate change	Human activities	Climate change	Human activities
0–20	53.3	8.3	35.3	3.6	91.2	0.7
20–40	23.0	4.9	42.1	2.8	6.7	0.4
40–60	11.5	12.0	16.7	20.1	1.0	1.2
60–80	4.1	25.7	2.6	41.6	0.4	9.0
≥ 80	8.1	49.1	3.3	31.9	0.7	88.7

4 Discussion

4.1 Data and method evaluation

Due to the low spatial and spectral resolution, it is challenging to estimate sparse desert vegetation coverage in ultra-arid regions (Fensholt and Proud, 2012). Compared with GT-NDVI and AVHRR-NDVI data, the 250 m MODIS NDVI product is able to afford more accurate information on the land surface. MODIS-based vegetation indices are optimally for distinguishing the differences between sparse and dense vegetation areas. Therefore, the vegetation information described by the MODIS NDVI vegetation index (250 m spatial resolution) is suitable for monitoring the fragmented landscapes in drylands (Dubovyk *et al.*, 2013) and provides a data source for evaluating changes in regional vegetation. The Theil–Sen median trend analysis method and the Mann–Kendall test were used to explore

the vegetation sequence reflecting the trend of each pixel. This combinatorial analysis is more advantageous than the linear regression approach. The main advantages are that the data need not follow a specific distribution, the ability to avoid errors is strong, and the significance level test has a solid statistical theoretical basis. Therefore, we applied this combination to examine vegetation trends in this study area, which is more scientific and reliable than the techniques used by previous studies.

4.2 Vegetation dynamics and response to climatic driving factors

We determined that the vegetation in the study area has increased for over twenty years. These results were consistent with those of studies involving the global arid zone (Pinzon and Tucker, 2014), Eurasian continent (Piao *et al.*, 2011), and others (Man *et al.*, 2008; Li *et al.*, 2017; Zhao *et al.*, 2021). Our field investigations also demonstrated that the deserts are significantly greening (Figures 9–12). Although there were seasonal differences between our

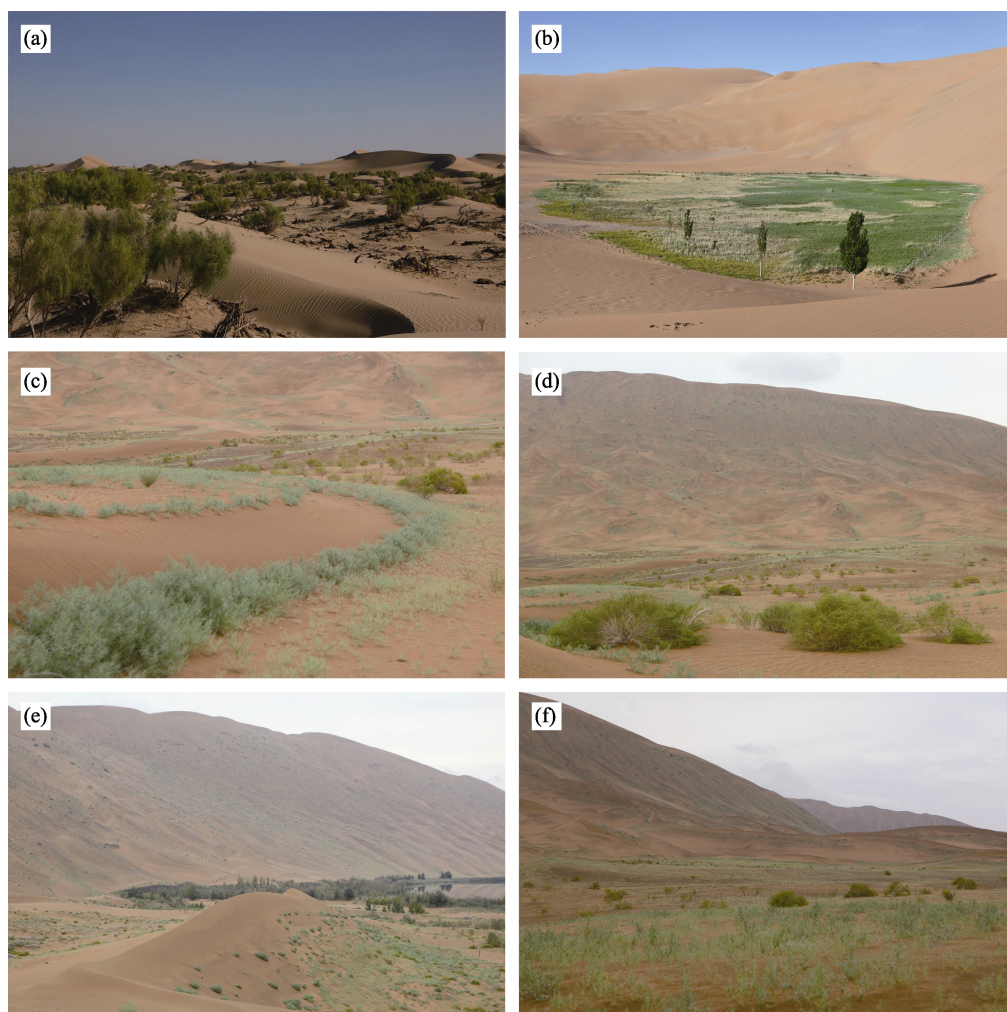


Figure 9 Vegetation landscapes in the Badain Jaran Desert: (a) *Haloxylon ammodendron* forest; (b) the oasis in the hinterland of the desert; and (c), (d), (e), and (f) inter-dune vegetation with *Agriophyllum sphaerocephala* and *Artemisia sphaerocephala* in September 2019



Figure 10 Vegetation and landscapes in the Mu Us Sandy Land (a) and (c): the Ming Great Wall in Xingwuying during April 2005; (b) and (d): the Ming Great Wall in Xingwuying during August 2018; (e) Chaganbala ancient city during October 2003; and (f) Chaganbala ancient city during October 2018

photos (Figures 9a, 9b and Figures 9c, 9d), the vegetation coverage has increased, and the ecology and environment have improved considerably. The NDVI in the study area was significantly increased, as confirmed by the remote sensing data and fieldwork.

The climate has presented warming and wetting trends over the 20-year test period. This corresponds with findings proposed by Shi *et al.* (2007) where the climate in northwest China transformed from warming–drying to warming–wetting. Previous research has suggested that the rising in temperature could lead to a significant increase in NDVI (Zhou *et al.*, 2015). However, in our study, the response of the NDVI was stronger for precipitation than temperature, and the relationships between the NDVI and air temperature were not significant. The temperature exhibited an inhibitory effect on vegetation growth in some areas largely because these regions were predominantly located in arid areas. Elevated temperatures would raise evapotranspiration and reduce water use efficiency, increasing the pressure

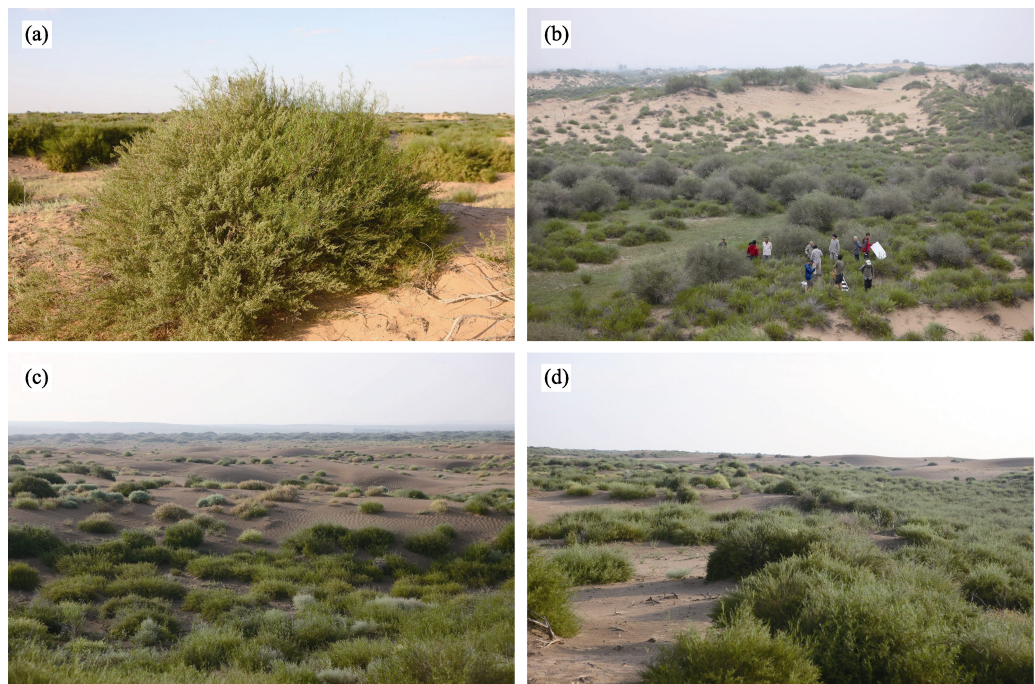


Figure 11 Vegetation and landscapes in the Mu Us Sandy Land in August 2012 (a), (b), (c), and (d)

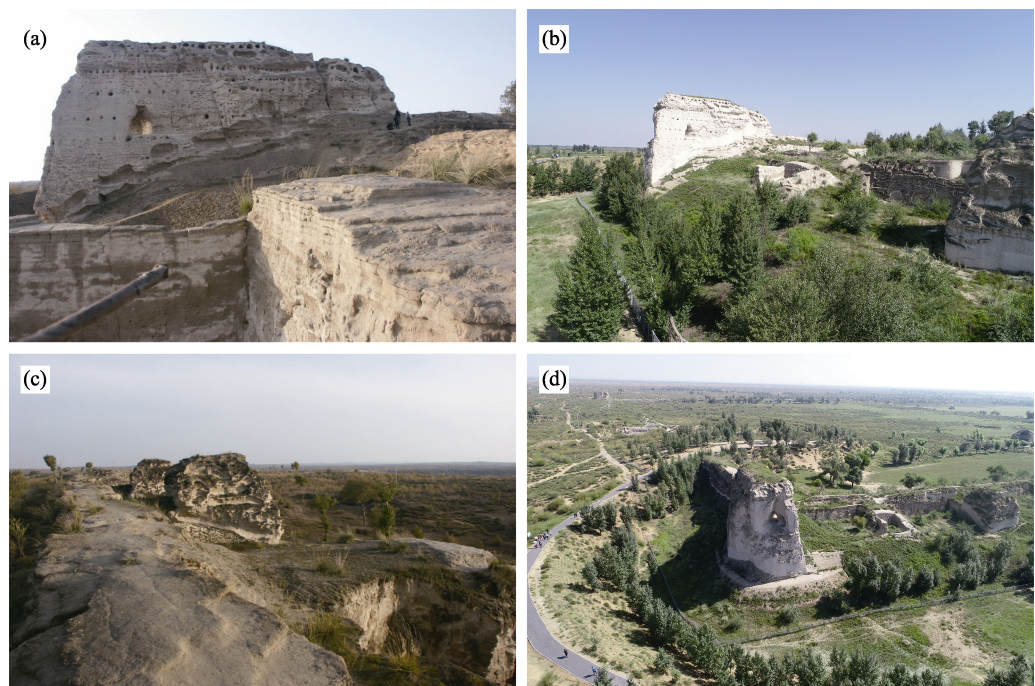


Figure 12 Vegetation and landscapes in Tongwan city in the Mu Us Sandy Land: (a) and (c) investigated in October 2003; (b) and (d) investigated in August 2018

on the vegetation and limiting vegetation growth, especially the growth of shrubs (Barber *et al.*, 2000; Nemani *et al.*, 2003; Matthias *et al.*, 2015; Wu *et al.*, 2015; Lu *et al.*, 2022).

Therefore, climate warming can promote vegetation growth in ecologies with limited temperatures, but it has the opposite effect on semi-arid and arid ecosystems where water is scarce. Precipitation is the dominant factor for vegetation greening in arid and semi-arid areas (Tao *et al.*, 2018). This was also supported by the results of our study. In addition to the climatic variable, the role of human activities on NDVI cannot be excluded. Human factors play an increasingly important role in vegetation dynamics in China and worldwide (Sun *et al.*, 2015; Tian *et al.*, 2021). The results of this study demonstrate that the average contribution from human activities to NDVI changes was $> 70\%$. Ecosystem conservation policies contribute more toward vegetation change than climatic factors do. Since the 1990s, large ecological conservation and restoration projects have been carried out, such as the “Three Norths Shelter Forest Program,” “Combating of Desertification Program,” “Natural Forests Conservation Program,” and “Grain for Green Project,” which have significantly affected vegetation restoration. Vegetation in these regions has been restored because of the combined influence of ecological engineering and natural elements. Based on the different vegetation change-driven zones, we suggest the implementation of grazing bans and afforestation policies in non-climate-driven desert areas while implementing enclosure measures in climate-driven areas. In desert areas, where water resources are limited, vegetation restoration may exacerbate local drought, aggravating the water contradiction between humans and ecosystems (Menz *et al.*, 2013; Feng *et al.*, 2016; Zhang *et al.*, 2018). Therefore, when undertaking vegetation restoration activities in areas with poor water conditions, its impact on regional water resource security should be examined. Vegetation should be appropriately increased in these zones according to climate change drivers (Jiang *et al.*, 2017; Zhao *et al.*, 2017).

The average rate of increase for the NDVI values in the MUSL was 0.61/10 a. This was higher than the mean rate of increase at 0.34/10 a observed in China, which indicates that the vegetation recovers more rapidly than in other areas, and the effect of ecological engineering is more pronounced. In the three areas, the mean value and the trend of the NDVI growth rate in the MUSL were the highest. The differences in natural background, socioeconomic development, and ecological restoration project investment in these three regions lead to differences in vegetation restoration status. Specifically, the MUSL has not been a barren land since ancient times. This area contains abundant water resources and high grass coverage. However, under the influence of the gradual expansion of human activities, over-reclaiming, over-grazing and over-cutting have led to continuous desertification (Runnstrom, 2003). Compared with the BJD and TD, the MUSL has superior natural conditions, better hydrothermal conditions, as indicated by the higher precipitation in the MUSL (312.9 mm) than in the BJD (82.8 mm) and TD (143.8 mm) in this study, and more kinds of vegetation. The relatively abundant surface water and groundwater in most parts of the MUSL also play vital roles in the improvement of vegetation conditions (Wu, 2001). The Chinese Government has implemented several large-scale ecological protection projects in these regions. Specific ecological engineering measures for each region are as follows. In the Alxa comprehensive desert control zone, the local government strengthened the construction of desertified land closure protection zones, built a wind break and sand fixation forest system combining trees, shrubs, and grasses, accelerated the development of clasp forests in the BJD and TD, and control desert extension by relying on the key projects. To

prevent and control desertification and protect oases, afforestation intensified by air seeding, sand sealing, and artificial forestation strengthen the construction of the Juyanhai wetland, *Populus euphratica* forest, and other nature reserves and desert parks. One of the longest lasting sand-binding projects is located in Shapotou region. It was established in 1956–1991 to mitigate desertification and prevent the Baotou–Lanzhou Railway from being buried in sand. Straw checkerboards were used to stabilize the dunes, and drought-resistant shrubs were planted in this site. The regional ecological environment, including the soil physical and chemical properties as well as the diversity of the animal and plant species, has been significantly improved since the establishment of sand-binding vegetation (Yang *et al.*, 2014). In the MUSL, biological and engineering measures, such as afforestation by air seeding and fencing of sandy areas, have been implemented. The structure of livestock in pastoral areas has also been affected by the local prohibition of grazing, rest grazing, rotational grazing. The grazing pressure of grassland in the sandy area was relieved, which had a positive impact on the improvement of vegetation growth in MUSL. A green forest belt with *Pinus sylvestris* as the main body was established in the hinterland of the desert, gradually forming a solid green ecological barrier in the MUSL. In addition, sand dunes were leveled, sand barriers were established, and other sand control techniques were applied (Xu *et al.*, 2018).

4.3 Uncertainties in the attribution of observed NDVI changes

Quantitative assessment of the relative contribution of human activities and climate change to NDVI changes is a challenging task. However, this is necessary to identify the driving factors of NDVI. There have been relatively few quantitative analyses of the climatic and human factors that influence the NDVI in these regions. We used residual trend analysis to isolate the effect that climatic change and human activities have on vegetation. Our residual analysis indicated that human activities played had a considerable effect on vegetation coverage and were the main driving factors for changes in vegetation cover. Although this is a practical and feasible quantitative analysis approach, it is characterized by limitations and uncertainties. The main problems include several factors. 1) When establishing the multiple regression equation between the NDVI and climatic factors, we did not consider all the climatic factors. It is difficult to select the most suitable climatic factors to clarify variation in the vegetation. The response of NDVI to climate change experiences lag and accumulation. Therefore, the time scale of lag and accumulation length needs to be refined. 2) We could only obtain data from areas where human activities promoted vegetation coverage and those where human activities lead to a decrease in vegetation. A large quantity of data and field-work are required to document the different types of human activities. The results of the residual trend method were in line with other research findings, however, the driving mechanisms of vegetation change require further study. In the absence of detailed socio-economic statistics, we calculated the human activities collectively. However, the response mechanism of vegetation changes to human activities is complex, especially since the 21st century. The range and intensity of human activities are gradually expanding, including land-use changes, conversion of farmland to forests, and adjustments to the agricultural structure. Therefore, the next step could be extracting and quantifying the impacts of human activity. New methods and tools should be applied to quantify the impact of human activities on NDVI.

4.4 Limitations and prospects

Owing to the limited spatial and temporal resolution of the NDVI products and gridded climate data, we only paid attention to the NDVI trends and their reactions to climate changes and human activities. However, we did not take into account their influences on the diverse growth period of various vegetation types and on evaluating vegetation responses to extreme climate, such as single maximum and minimum precipitation. A range of results may also be obtained because various NDVI data sources have different resolutions. However, this study did not use multiple NDVI datasets. Research groups should establish future collaboration for more precise results. We studied the correlation between the NDVI and climate indices on an inter-annual scale and the lag in the influence of the climatic factors on NDVI were not analyzed. To better understand the temporal lag effect of NDVI responses on climatic factors at different time scales, further research can be performed. Thus, the results of this study reflect changes in vegetation across the survey region and the relationship between climate change and human activities, which can offer theoretical support for vegetation restoration and ecological building in this region and the entire country.

5 Conclusions

Based on MODIS NDVI and climatic data, the trend, correlation, and residual analyses were used to examine the spatiotemporal patterns in the NDVI over the BJD, TD, and MUSL regions, as well as its relationship with climate variation and human activities. The following conclusions were obtained on the basis of our results and interpretation.

(1) Over the last 20 years (2001–2020), the NDVI in the study area has significantly increased and presented considerable spatial heterogeneity. Vegetation increased in the BJD (mainly in the southeast) and TD (mainly in the southeast, northeast, and northwest) areas. There were significant improvements in most parts of the MUSL. The improved vegetation area was greater than the degraded area.

(2) Climate change and human activities contributed to NDVI change. Their relative effects on variation in the vegetation had pronounced spatial differences. Precipitation was the main climatic factor controlling changes in NDVI. Human activities were the dominant factor that induced an increase in the NDVI, with a relative contribution of $>-70\%$. The implementation of ecological restoration projects has facilitated vegetation restoration and improved the regional environment.

References

- Barber V A, Juday G P, Finney B P, 2009. Reduced growth of Alaskan white spruce in the twentieth century from temperature-induced drought stress. *Nature*, 405(6787): 668–673.
- Chen C, Park T J, Wang X *et al.*, 2019. China and India in greening of the world through land-use management. *Nature Sustainability*, 2(2): 122–129.
- Dong Z, Wang T, Wang X, 2004. Geomorphology of the megadunes in the Badain Jaran Desert. *Geomorphology*, 60(1): 191–203.
- Du J, Quan Z, Fang S *et al.*, 2019. Spatiotemporal changes in vegetation coverage and its causes in China since the Chinese economic reform. *Environmental Science and Pollution Research*, 27(1): 1144–1159.
- Dubovyyk O, Menz G, Conrad C *et al.*, 2013. Spatio-temporal analyses of cropland degradation in the irrigated

- lowlands of Uzbekistan using remote-sensing and logistic regression modeling. *Environmental Monitoring & Assessment*, 185(6): 4775–4790.
- Eastman J, Florencia S, Elia M *et al.*, 2013. Global trends in seasonality of normalized difference vegetation index (NDVI), 1982–2011. *Remote Sensing*, 5(10): 4799–4818.
- Evans J, Geerken R, 2004. Discrimination between climate and human-induced dry land degradation. *Journal of Arid Environments*, 57(4): 535–554.
- Feng X, Fu B, Piao S *et al.*, 2006. Revegetation in China's Loess Plateau is approaching sustainable water resource limits. *Nature Climate Change*, 6(11): 1019–1022.
- Fensholt R, Proud S R, 2012. Evaluation of earth observation based global long term vegetation trends: Comparing GIMMS and MODIS global NDVI time series. *Remote Sensing of Environment*, 119: 131–147.
- Forkel M, Migliavacca M, Thonicke K *et al.*, 2015. Codominant water control on global interannual variability and trends in land surface phenology and greenness. *Global Change Biology*, 21(9): 3414–3435.
- Forzieri G, Alkama R, Miralles D G *et al.*, 2017. Satellites reveal contrasting responses of regional climate to the widespread greening of Earth. *Science*, 356(6343): 1180–1184.
- Gao J, Jiao K, Wu S *et al.*, 2019. Investigating the spatially heterogeneous relationships between climate factors and NDVI in China during 1982 to 2013. *Journal of Geographical Sciences*, 29(10): 1597–1609.
- Guo Z, Wei W, Shi P *et al.*, 2020. Spatiotemporal changes of land desertification sensitivity in the arid region of Northwest China. *Acta Geographica Sinica*, 75(9): 1948–1965 (in Chinese)
- Hellden U, 2008. A coupled human-environment model for desertification simulation and impact studies. *Global and Planetary Change*, 64(3/4): 158–168.
- Holben B, 1986. Characteristics of maximum-value composite images from temporal AVHRR data. *International Journal of Remote Sensing*, 7(11): 1417–1434.
- Jiang L, Jiapaer G, Bao A *et al.*, 2017. Vegetation dynamics and responses to climate change and human activities in Central Asia. *The Science of the Total Environment*, 599/600 (Dec.): 967–980.
- Jin K, Wang F, Han J *et al.*, 2020. Contribution of climatic change and human activities to vegetation NDVI change over China during 1982–2015. *Acta Geographica Sinica*, 75(5): 961–974. (in Chinese)
- Justice C, Townshend J, 2002. Special issue on the moderate resolution imaging spectroradiometer (MODIS): A new generation of land surface monitoring. *Remote Sensing of Environment*, 83(1/2): 1–2.
- Kendall M, 1975. Rank Correlation Methods. London: Charles Griffen.
- Li S, Yan J, Liu X *et al.*, 2013. Response of vegetation restoration to climate change and human activities in Shaanxi-Gansu-Ningxia region. *Journal of Geographical Sciences*, 23(1): 98–112.
- Li Y, Cao Z, Long H *et al.*, 2017. Dynamic analysis of ecological environment combined with land cover and NDVI changes and implications for sustainable urban-rural development: The case of Mu Us Sandy Land, China. *Journal of Cleaner Production*, 142(2): 697–715.
- Liu C, Zhao W, Liu B *et al.*, 2019. Distribution characteristics and dynamic changes of vegetation in Badain Jaran Desert: Based on UAV and MODIS data. *Journal of Desert Research*, 39(4): 92–102. (in Chinese)
- Liu X, Zhu X, Pan Y *et al.*, 2016. Vegetation dynamics in Qinling-Daba Mountains in relation to climate factors between 2000 and 2014. *Journal of Geographical Sciences*, 26(1): 45–58.
- Liu Z, Dong Z, Wang J *et al.*, 2016. Vegetation characteristics in the marginal areas of the Badain Jaran Desert. *Journal of Desert Research*, 36(5): 1348–1356. (in Chinese)
- Lu X, Liang E, Babst F *et al.*, 2022. Warming-induced tripping points of Arctic and alpine shrub recruitment. *PNAS*. 119(9): e2118120119.
- Ma N, Wang N, Zhu J *et al.*, 2011. Climate change around the Badain Jaran Desert in recent 50 years. *Journal of Desert Research*, 31(6): 1541–1547. (in Chinese)
- Man D, Dong Z, Ji Y *et al.*, 2008. Seasonal vegetation change and sand-wind activity in southwest fringe of Tengger Desert. *Journal of Desert Research*, 28(6): 1029–1032. (in Chinese)
- Menz M, Dixon K W, Hobbs R J, 2013. Hurdles and opportunities for landscape-scale restoration. *Science*, 339(6119): 526–527.
- Mynel R B, Keeling C D, Tucker C J *et al.*, 1997. Increased plant growth in the northern high latitudes from 1981

- to 1991. *Nature*, 386(6626): 698–702.
- Neeti N, Eastman J R, 2011. A contextual Mann-Kendall approach for the assessment of trend significance in image time series. *Transactions in GIS: TG*, 15(5): 599–611.
- Nemani R R, Keeling C D, Hashimol H *et al.*, 2003. Climate-driven increased in global terrestrial net primary production from 1982 to 1999. *Science*, 300(5625): 1560–1563.
- Piao S, Wang X, Ciais P *et al.*, 2011. Changes in satellite-derived vegetation growth trend in temperate and boreal Eurasia from 1982 to 2006. *Global Change Biology*, 17(10): 3228–3239.
- Piao S, Wang X, Park T *et al.*, 2020. Characteristics, drivers and feedbacks of global greening. *Nature Reviews Earth & Environment*, 1(1): 14–27.
- Piao S, Yin G, Tian J *et al.*, 2015. Detection and attribution of vegetation greening trend in China over the last 30 years. *Global Change Biology*, 21(4): 1601–1609.
- Pinzon J, Tucker C J, 2014. A non-stationary 1981–2012 AVHRR NDVI13g time series. *Remote Sensing*, 6(8): 6929–6960.
- Qu S, Wang L, Lin A *et al.*, 2020. Distinguish the impacts of climate change and anthropogenic factors on vegetation dynamics in the Yangtze River Basin, China. *Ecological Indicators*, 108: 105724.
- Runnstrom M, 2003. Rangeland development of the Mu Us Sandy Land in semiarid China: An analysis using Landsat and NOAA remote sensing data. *Land Degradation & Development*, 14(2): 189–202.
- Sen P K, 1968. Estimates of the regression coefficient based on Kendall's tau. *Journal of the American Statistical Association*, 63(324): 1379–1389.
- Shao Q, Cao W, Fan J *et al.*, 2017. Effects of an ecological conservation and restoration project in the Three-River Source Region, China. *Journal of Geographical Sciences*, 27(2): 183–204.
- Shi Y, Shen Y, Kang E *et al.*, 2007. Recent and future climate change in northwest China. *Climatic Change*, 80(3/4): 379–393.
- Song X, Hansen M C, Stehman S V *et al.*, 2018. Global land change from 1982 to 2016. *Nature*, 560(7720): 639–643.
- Sun Y, Yang Y, Zhang L *et al.*, 2015. The relative roles of climate variations and human activities in vegetation change in North China. *Physics and Chemistry of the Earth, Parts A/B/C*: 87–88, 67–78.
- Tao J, Xu T, Dong J *et al.*, 2018. Elevation-dependent effects of climate change on vegetation greenness in the high mountains of southwest China during 1982–2013. *International Journal of Climatology*, 38(4): 2029–2038.
- Theil H, 1950. A rank-invariant method of linear and polynomial regression analysis. I, II, and III. *Proceedings of Koninklijke Nederlandse Akademie van Wetenschappen* 53: 386–392, 521–525, 1397–1412.
- Tian F, Liu L, Yang J *et al.*, 2021. Vegetation greening in more than 94% of the Yellow River Basin (YRB) region in China during the 21st century caused jointly by warming and anthropogenic activities. *Ecological Indicators*, 125: 107479.
- Tucker C J, Townshend J R, Goff T E, 1985. African land-over classification using satellite data. *Science*, 227(4685): 369–375.
- Wang C, Liang W, Yan J *et al.*, 2022. Effects of vegetation restoration on local microclimate on the Loess Plateau. *Journal of Geographical Sciences*, 32(2): 291–316.
- Wang T, 2003. Study on sandy desertification in China: 2. Contents of desertification research. *Journal of Desert Research*, 23(5): 1–6. (in Chinese)
- Wang X, Li Y, Wang X *et al.*, 2021. Temporal and spatial variations in NDVI and analysis of the driving factors in the desertified areas of northern China from 1998 to 2015. *Frontiers in Environmental Science*, 9: 633020.
- Wang Y, Shao M, Shao H, 2010. A preliminary investigation of the dynamic characteristics of dried soil layers on the Loess Plateau of China. *Journal of Hydrology*, 381 (1/2): 9–17.
- Wei W, Guo Z, Shi P *et al.*, 2021. Spatiotemporal changes of land desertification sensitivity in northwest China from 2000 to 2017. *Journal of Geographical Sciences*, 31(1): 46–68.
- Wei Z, Wang D, Zhang C, 2014. Response of vegetation cover to climate change and human activities in northwest China during 1999–2010. *Journal of Desert Research*, 34(6): 1665–1670. (in Chinese)

- Wu B, Ci L, 2002. Landscape change and desertification development in the Mu Us Sandland, northern China. *Journal of Arid Environment*, 50(3): 429–444.
- Wu D, Zhao X, Liang S *et al.*, 2015. Time-lag effects of global vegetation responses to climate change. *Global Change Biology*, 21(9): 3520–3531.
- Wu H, 2001. Study on process of desertification in Mu Us Sandy Land for last 50 years, China. *Journal of Desert Research*, 21(2): 164–169. (in Chinese)
- Xu Z, Hu R, Wang K *et al.*, 2018. Recent greening (1981–2013) in the Mu Us dune field, north-central China, and its potential causes. *Land Degradation & Development*, 29(5): 1509–1520.
- Yang H, Li X, Wang Z *et al.*, 2014. Carbon sequestration capacity of shifting sand dune after establishing new vegetation in the Tengger Desert, northern China. *Science of the Total Environment*, 478, 1–11.
- Yuan W, Li X, Liang S *et al.*, 2014. Characterization of locations and extents of afforestation from the Grain for Green Project in China. *Remote Sensing Letters*, 5(3): 221–229.
- Zhang K, Qu J, An Z, 2012. Characteristics of wind-blown sand and near-surface wind regime in the Tengger Desert, China. *Aeolian Research*, 6: 83–88.
- Zhang X, Wang N, Xie Z *et al.*, 2018. Water loss due to increasing planted vegetation over the Badain Jaran Desert, China. *Remote Sensing*, 10(1): 134.
- Zhao A, Zhang A, Lu C *et al.*, 2017. Spatiotemporal variation of vegetation coverage before and after implementation of Grain for Green Project in the Loess Plateau. *Ecological Engineering*, 104: 13–22.
- Zhao C, Cheng Y, Li Y *et al.*, 2021. Land use/cover change of an artificial vegetation system in the northeastern edge of Tengger Desert. *Journal of Arid Land Resources and Environment*, 35(6): 131–138. (in Chinese)
- Zhou D, Zhao X, Hu H *et al.*, 2015. Long-term vegetation changes in the four mega-sandy lands in Inner Mongolia, China. *Landscape Ecology*, 30(9): 1613–1626.
- Zhou Y, Zhang L, Fensholt R *et al.*, 2015. Climate contributions to vegetation variations in central Asian drylands: Pre- and post-USSR collapse. *Remote Sensing*, 7(3): 2449–2470.
- Zhu J, Wang N, Chen H *et al.*, 2010. Study on the boundary and the area of Badain Jaran Desert based on remote sensing imagery. *Progress in Geography*, 29(9): 1087–1094.
- Zhu Z, Wu Z, Liu S, 1980. An Outline of Chinese Deserts. Beijing: Science Press, 71–73.